View metadata, citation and similar papers at core.ac.uk

brought to you by CORE

provided by Jefferson Digital Commons

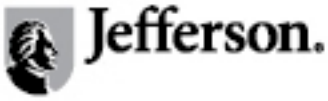

Thomas Jefferson University
Jefferson Digital Commons

Department of Biochemistry and Molecular Biology Faculty Papers

Department of Biochemistry and Molecular Biology

October 2004

Inhibition of glucocorticoid-induced apoptosis by targeting splice variants of *BIM* mRNA with small interfering RNA and short hairpin RNA.

Marc T. Abrams
Thomas Jefferson University, marc.abrams@jefferson.edu

Noreen M. Robertson
Thomas Jefferson University, Noreen.Robertson@jefferson.edu

Kyonggeun Yoon
Thomas Jefferson University, Kyonggeun.Yoon@jefferson.edu

Eric Wickstrom
Thomas Jefferson University, eric@tesla.jci.tju.edu

Let us know how access to this document benefits you

Follow this and additional works at: https://jdc.jefferson.edu/bmpfp

Part of the Medical Biochemistry Commons

Recommended Citation

Abrams, Marc T.; Robertson, Noreen M.; Yoon, Kyonggeun; and Wickstrom, Eric, "Inhibition of glucocorticoid-induced apoptosis by targeting splice variants of *BIM* mRNA with small interfering RNA and short hairpin RNA." (2004). *Department of Biochemistry and Molecular Biology Faculty Papers.* Paper 3.
https://jdc.jefferson.edu/bmpfp/3

This Article is brought to you for free and open access by the Jefferson Digital Commons. The Jefferson Digital Commons is a service of Thomas Jefferson University's Center for Teaching and Learning (CTL). The Commons is a showcase for Jefferson books and journals, peer-reviewed scholarly publications, unique historical collections from the University archives, and teaching tools. The Jefferson Digital Commons allows researchers and interested readers anywhere in the world to learn about and keep up to date with Jefferson scholarship. This article has been accepted for inclusion in Department of Biochemistry and Molecular Biology Faculty Papers by an authorized administrator of the Jefferson Digital Commons. For more information, please contact: JeffersonDigitalCommons@jefferson.edu.

Inhibition of glucocorticoid-induced apoptosis by targeting the major splice variants of *BIM* mRNA with siRNA and shRNA

Marc T. Abrams[1], Noreen M. Robertson[1†], Kyonggeun Yoon[1,2] and Eric Wickstrom[1,3]*

[1]Department of Biochemistry and Molecular Pharmacology, [2]Department of Dermatology and Cutaneous Biology, and [3]Kimmel Cancer Center

Thomas Jefferson University

Philadelphia, Pennsylvania 19107, U.S.A.

***To whom correspondence should be sent:** Dr. Eric Wickstrom, Department of Biochemistry and Molecular Pharmacology, Thomas Jefferson University, 233 S. 10th Street, Suite 219, Philadelphia PA 19107. Phone: 215.955.4578, Fax: 215.955.4580. email: eric@tesla.jci.tju.edu

Running title: Bim and glucocorticoid-induced apoptosis

Key words: apoptosis, Bim, glucocorticoid, siRNA, lentivirus, triamcinolone

[†]Present Address: A. J. Drexel Institute of Basic and Applied Protein Science, Drexel University School of Medicine, Philadelphia, PA 19102

Grant support: DOE/BER ER63055 to E. W.

Summary

Glucocorticoids (GCs) induce apoptosis in lymphocytes and are effective agents for the treatment of leukemia. The activated glucocorticoid receptor (GR) initiates a transcriptional program leading to caspase activation and cell death, but the critical signaling intermediates in GC-induced apoptosis remain largely undefined. We have observed that GC induction of the three major protein products of the Bcl-2 relative Bim (BimEL, BimS and BimL) correlates with GC sensitivity in a panel of human pre-B acute lymphoblastic leukemia (ALL) cell lines. To test the hypothesis that Bim facilitates GC-induced apoptosis, we reduced *BIM* mRNA levels and Bim protein levels by RNA interference (RNAi) in highly GC-sensitive pre-B ALL cells. Reducing Bim proteins by either electroporation of synthetic siRNA duplexes or lentiviral-mediated stable expression of shRNA inhibited activation of caspase-3 and increased cell viability following GC exposure. We also observed that the extent of GC resistance correlated with siRNA silencing potency. siRNA duplexes that reduced only BimEL or BimEL and BimL (but not BimS) exhibited less GC resistance than a potent siRNA that silenced all three major isoforms, implying that induction of all three Bim proteins contributes to cell death. Finally, the modulation of GC-induced apoptosis caused by Bim silencing was independent of Bcl-2 expression levels, negating the hypothesis that the ratio of Bim to Bcl-2 regulates apoptosis. These results offer evidence that induction of Bim by GC is a required event for the complete apoptotic response in pre-B ALL cells.

Introduction

Glucocorticoids (GCs)[1] are steroid hormones that maintain physiological homeostasis. Synthetic GCs such as dexamethasone and triamcinolone acetonide (TA) are widely prescribed pharmaceuticals for indications ranging from inflammation to cancer. GCs induce apoptosis in numerous lymphoid and myeloid tissues, and have been successful in the treatment of childhood leukemias (1). The mechanism of GC-induced apoptosis involves the hallmarks of the intrinsic pathway of apoptosis: release of cytochrome c and Smac from the mitochondria and activation of caspase-9 (2). Determining the molecular trigger(s) that commit the cell to activation of intrinsic apoptosis might enable strategies to combat GC-resistant leukemias. Precursor B-cell (pre-B) acute lymphoblastic leukemia (ALL) is the most common childhood cancer and a useful model to investigate the mechanism of GC-induced apoptosis (3).

GC signaling occurs through the glucocorticoid receptor (GR), a nuclear receptor superfamily member that dissociates from a large Hsp70-containing complex and translocates to the nucleus upon GC binding, reviewed in (4). The activated GR initiates a tissue-specific transcriptional program through both direct DNA binding and interaction with other transcription

[1] Abbreviations: ALL, acute lymphoblastic leukemia; BH3, Bcl-2 homology domain 3; GC, glucocorticoid; GFP, green fluorescent protein; GR, glucocorticoid receptor; DAPI, 4',6-Diamidino-2-phenylindole; μF, microfarads; PBS, phosphate-buffered saline; 7-AAD, 7-aminoactinomycin D; TA, triamcinolone acetonide; RNAi, RNA interference; RT-PCR, reverse transcriptase-polymerase chain reaction; siRNA, small-interfering RNA; shRNA, short hairpin RNA; Smac, second mitochondria-derived activator of caspase.

factors. Numerous studies with actinomycin D and cycloheximide have demonstrated that new transcription and protein synthesis, respectively, are required for GC-induced apoptosis (5,6). Microarray profiling has shown that a short GC exposure induces or represses transcription of over 100 genes by a factor of 3-fold or greater in multiple models of GC-induced apoptosis (7-9). Among these genes are universal regulators of intrinsic apoptosis, such as *BCL2,* and *BIM*, a gene encoding several splice variants of the related BH3 (Bcl-2 homology region 3)-domain containing protein Bim (7,9). GC represses *BCL2* transcription, but induces *BIM* transcription. Lymphocytes containing overexpressed (7) or high endogenous levels (10) of Bcl-2 protein are partially GC-resistant, underscoring the significance of intrinsic pathway regulation in GC signaling. Bim protein is in the"BH3-only" (Bcl-2 homology-3) subset of Bcl-2 relatives, a group that also includes Bid, Bad, Puma, and Noxa. BH3-only proteins are transcriptionally activated, post-translationally modified or released from sequestration in response to death stimuli, and promote apoptosis by interacting with Bcl-2 family members that contain multiple BH domains (BH1-BH4), reviewed in (11).

Bim is a critical regulator of immune cell homeostasis as well as apoptosis in several tissue types, and has been recently investigated in preclinical models as a potential cancer therapeutic (12,13). Mice lacking Bim contain strikingly high numbers of leukocytes and eventually succumb to autoimmune disease (14). Importantly, thymocytes isolated from these mice demonstrate a delayed apoptotic response to the GC dexamethasone (14). Loss of a single allele of *BIM* accelerated the rate of murine c-*myc*-induced lymphoma development, leading to classification of Bim as a tumor suppressor protein (15). Bim expression is induced by growth factor withdrawal (16,17), T-cell receptor ligation (18), paclitaxel treatment (19) and forced growth in suspension (20,21) in various cell types, suggesting that transcriptional regulation of Bim is an upstream event in apoptosis induced by diverse stimuli. Finally, lowering *BIM* mRNA

by RNAi causes partial protection against apoptosis induced by the drugs paclitaxel (19) and imitinib (22), as well as apoptosis induced by forced suspension culture (anoikis) (20,21).

The *BIM* gene is transcribed as three major spice variants: *BIM EL*, *BIM L*, and *BIM S*, encoding the functionally-distinct proteins BimEL, BimL, and BimS, respectively (23). BimS protein has been widely reported to be the most strongly pro-apoptotic of the three, although there may be exceptions (16). Only BimEL is likely to be regulated by phosphorylation and caspase-3 cleavage (24). Both BimEL and BimL (but not BimS) may be sequestered by LC8, a subunit of the dynein motor complex (25), though the significance of this interaction has recently been questioned (26).

Previous studies in our laboratory (7) and others (9,27) have led to speculation that transcriptional induction of Bim is required for GC-induced apoptosis. Only correlative evidence has thus far been generated in leukemic cells. In order to test this hypothesis directly, we used RNA interference (RNAi) (28) to reduce *BIM* mRNA levels and found that both synthetic siRNAs and lentiviral-expressed shRNAs rendered human 697 pre-B ALL cells partially resistant to GC and inhibited GC-induced caspase-3 activity. Using splice variant-specific siRNAs, we found that all three major isoforms contribute to GC-induced apoptosis. Finally, we demonstrate that the Bim/Bcl-2 ratio is not a critical parameter in this pathway, suggesting that Bim functions primarily in a Bcl-2-independent manner in pre-B ALL cells.

Materials and Methods

Cell culture and reagents. The pre-B ALL cells lines were cultured in RPMI-1640 medium (Invitrogen, Carlsbad, CA) supplemented with 10% fetal bovine serum (FBS, Invitrogen). Nalm-6, Kasumi-2, and Kopn-8 cells were acquired from DSMZ (Braunschweig, Germany). Triamcinolone acetonide (TA), polybrene, and all other reagents were purchased from Sigma (St.

Louis, MO) unless otherwise indicated. Horseradish peroxidase-conjugated secondary antibodies were obtained from Santa Cruz Biotechnology (Santa Cruz, CA).

Electroporation of siRNA. siRNAs were purchased from Dharmacon, Inc. (Lafayette, CO). The sense strand sequences of the RNA duplexes used were as follows: Control siRNA (firefly luciferase, 5'-CGUACGCGGAAUACUUCGA(dTdT)-3'); *KIF11* (5'-AACUGAAGACCUGAAGACAAU(dTdT)-3'); *BIM*#1 (5'-ACCGAGAAGGUAGACAAUU(dTdT)-3'), *BIM*#2 (5'-CUACCUCCCUACAGACAGA(dTdT)-3'); *BIM EL* (5'-CUCGAUCCUCCAGUGGGUA(dTdT)-3'); *BIM EL* + *BIM L* (5'-CAGCACCCAUGAGUUGUGA(dTdT)-3'); *BCL2*#1 (5'AGAUAGUGAUGAAGUACAUUU-3'); *BCL2*#2 (5'-GAAGUACAUCCAUUAUAAGUU-3'); *BCL2*#3 (5'-GGGAGAUAGUGAUGAAGUAUU-3'). Cells were washed twice with phosphate buffered saline (PBS) and resuspended in serum-free RPMI-1640 medium containing 25 mM HEPES (no phenol red or antibiotics) at 10^7 cells/mL. A 200 µL aliquot of cells was added to a 0.2 cm gap electroporation cuvet (Bio-Rad, Hercules, CA), along with 10 µL of a 20 µM stock of siRNA, then incubated at room temperature for 20 minutes. Cells were then electroporated with a Bio-Rad Gene Pulser using the indicated conditions, incubated for an additional 20 min and added to 2 mL of the above medium (excluding aggregated cell debris) supplemented with 10% FBS. Thus, the final concentration of siRNA is 100 nM following electroporation. The standard condition of 500 µF capacitance (see Results) achieved a pulse length of 7-8 ms. Vehicle (0.05% ethanol) or TA was added after the indicated recovery times.

Cell cycle analysis and viability assays. Electroporated and drug treated 697 cells were harvested, washed with PBS and fixed with 70% ethanol. After fixing for 18 h at 4ºC, cells were

collected by centrifugation and resuspended in 1 mL of staining solution containing 50 μg/mL propidium iodide, 1 mg/mL RNase A and 1 mg/mL glucose in PBS. Cells were analyzed for DNA content using a Beckman Coulter XL flow cytometer after 2 h of staining. 10,000 cells were counted per sample. Percentages of cells in sub-G0 or G2/M cell cycle fractions were determined using WinMDI software (Scripps Research Institute, La Jolla, CA). Trypan blue exclusion assays were performed in triplicate, counting >200 cells per sample.

Immunoblot analysis. Cells were washed once in PBS and lysed with RIPA buffer containing 1× Complete Protease Inhibitors (Roche, Indianapolis, IN). 30-50 μg of each whole cell extract was electrophoresed on Novex 12% Tris-Gly PAGE gels (Invitrogen) and transferred to nitrocellulose membranes. Immunoblots were performed using antibodies against Bim (1:20000 dilution, cat. # 202000, Calbiochem, San Diego, CA), Bcl-2 (1:10000, clone 100, Upstate Biotechnology, Lake Placid, NY), and GAPDH (1:20000, clone 6C5, Research Diagnostics, Flanders, NJ) using standard methods, and detected using chemoluminescent horseradish peroxidase substrates (Pierce, Rockford, IL). Densitometry analyses were performed by generating net intensity values using Kodak 1-D software (Rochester, NY).

RT-PCR. Total RNA was purified using RNeasy columns (Qiagen, Valencia, CA). RT-PCR was performed in 50 μL reactions using 100 ng RNA, 0.5 μM of each primer and an annealing temperature of 53ºC for 25 cycles. All other PCR conditions and reagents were supplied and recommended by the manufacturer's protocol for the Titan One-Step System (Roche). Primer sequences for *BIM* were (forward: 5'-GAGAAGGTAGACAATTGCAG-3'; reverse: 5'-GACAATGTAACGTAACAGTCG-3') and for *GAPDH* were (forward: 5'-CACCCATGGCAAATTCCATG-3' and reverse: TCTAGACGGCAGGTCAGGT-3').

Caspase analysis. For the caspase-3 substrate cleavage assay, one transfection was performed for each data point. Cells were washed with PBS, lysed and assayed in a 96-well plate using the EnzCheck Caspase-3 Assay Kit (Molecular Probes, Eugene, OR). Fluorescence was measured at emission and excitation settings of 485 nm/530 nm with a Bio-Tek FL600 plate reader (Winooski, VT). For immunofluoresence, 50,000 cells were spun onto microscope slides, fixed and permeabilized with 4% paraformaldehyde/0.1% Triton X-100, immunostained with anti-active caspase-3 antibody diluted 1:50 (Cell Signaling Technology, Beverly, MA), and counterstained with DAPI. Fluorescent detection was performed with the Vector Laboratories biotin/avidin system (Burlingame, CA) and AlexaFluor 488 (Molecular Probes, Eugene, OR).

Lentivirus generation and infection. The lentiviral transfer and packaging vectors were a generous gift from Dr. Xiao-Feng Qui. Lentivirus production was conducted by co-transfection of HEK293T cells with four plasmids: packaging defective helper construct (pMDLg/pRRE, 3 μg), a Rev-expressing construct (pRSV-Rev, 3 μg), a construct expressing a heterologous envelope protein (pCMV-VSVg, 5 μg), and a transfer vector harboring a specific shRNA sequence under control of the H1 RNA polymerase III promoter (pH1UG/Luc-shRNA or pH1UG/Bim-shRNA, 10 μg). Briefly, 3 x 10^6 HEK293T cells were seeded on 10 cm plates 24 h before transfection. For each shRNA, 100 μL of Fugene-6 (Roche) was combined the four plasmids in 3 mL serum free RPMI-1640 medium. The mixture was added dropwise onto the cells after a 30 min incubation and the cells were analyzed for green fluorescent protein (GFP) expression by fluorescence microscopy after 24 h. At 48 h, virus containing cell supernatants were collected and centrifuged twice to eliminate transfer of cells. shRNA-encoding pH1UG vectors were created by cloning annealed complementary oligonucleotides into BamH1 and Xho1 sites at the 3' of the H1 RNA Polymerase III promoter. The coding strand sequences of the shRNA-encoding oligonucleotides are as follows: Luciferase control (5'-

GATCCCCCGTATGCGGAATACTTTGATTCAAGAGATCGAAGTATTCCGCGTACGTTT TTC-3'); and *BIM* (5'-GATCCCCGACTGAGAAGGTAGATAATTTTCAAGAGAAATTGTCTACCTTCTCGGTCT TTTTC-3'). The *BIM* shRNA sequence used was modeled after the *BIM*#1 siRNA sequence. The 697 cells were infected by adding 1 mL viral supernatant supplemented with 4 μg/mL polybrene to 5 x 10^4 cells in 24 well plates. Viral supernatant was replaced with standard growth medium after 24 h, and infection efficiency was monitored by GFP expression after 48 h. Viral titers were calculated by counting GFP-positive cells after infecting with serial dilutions of viral supernatant.

Northern analysis. Total RNA was prepared from shRNA-expressing cell lines using Tri reagent (Sigma) according to the vendor's protocol. 30 μg of RNA were electrophoresed on a TBE-urea 15% acrylamide gel (Invitrogen) and transferred to a Zeta Probe nitrocellulose membrane (Bio-Rad, Hercules, CA). The membranes were UV cross-linked and probed with an end-labeled Bim antisense probe (5'-[^{32}P]AATTGTCTACCTTCTCGGTC-3') at 42ºC for 18 h. For the two hybridization control oligonucleotides (perfect match and 2-base mismatch), the two complementary *BIM* shRNA-encoding oligonucleotides were used since wobble base-pairing in the shRNA design (29) created two mismatches in the sense sequence of the coding strand oligonucleotide.

Results

The pro-apoptotic Bcl-2 relative Bim has been shown to be upregulated by GC in GC-sensitive lymphocytes, suggesting that Bim may function as an early sensor for intrinsic apoptosis (7,9,27). To determine if there is a correlation between Bim induction and GC

sensitivity in human pre-B ALL cells, we monitored a panel of human pre-B ALL cell lines for viability in response to the potent GC, triamcinolone acetonide (TA) after 48 h and 72 h exposures (Fig. 1a,b). Significant cell death was observed in the cell line 697 at low doses (5 nM) after 48 h, but the other lines tested (Kasumi-2, Kopn-8, and Nalm-6) showed no effect after 48 h and only slight (Kasumi-2, Kopn-8) or moderate (Nalm-6) cell death at the 72 h time point. We then compared the effect of TA on Bim protein levels in the sensitive and resistant cells (Fig 1c). We observed that the three major Bim proteins (BimEL, BimL, and BimS) (23) increased after 24 h in the 697 cells but not in the other pre-B ALL cell lines. In addition, basal levels of the Bim proteins were low or undetectable in the GC-resistant lines. To further explore the kinetics of Bim induction by GC, the 697 cells were also exposed to GC for shorter time points, showing rapid upregulation of the three Bim proteins after a 4 or 8 h exposure to 100 nM TA. Taken together, these data suggest that Bim expression and induction is a factor in determining the pro-apoptotic response to GC in pre-B ALL.

We then sought to reduce Bim expression in 697 cells by RNAi. Use of synthetic short-interfering RNA duplexes (siRNAs) has not been widely reported for lymphocytes, primarily due to the technical difficulty of nucleic acid transfection in non-adherent cultures. It has previously been shown that, for lymphocytes, electroporation is a more efficient delivery method for synthetic nucleic acids than liposome-mediated transfection (30). However, the cytotoxicity caused by the cellular stress of electroporation has often been too significant to perform downstream viability measurements. It has previously been reported (30) that an siRNA against the *KIF11* gene, which encodes the mitotic kinesin KSP (also known as Eg5), is an effective tool to optimize transfection conditions due to its ability to induce mitotic block. In order to determine conditions for electroporating siRNAs into human 697 pre-B lymphocytes, we tested several RNA concentrations and capacitance settings using a *KIF11*-targeting siRNA. After 48 hours, cell cycle analysis was performed using propidium iodide staining and flow cytometry.

Under optimized settings (220 V/500 μF), the percentage of cells blocked in the G2/M stage was two-fold higher for the KSP siRNA as compared to a control siRNA (Fig 2a), indicating that the level of transfection was sufficient to explore biological phenotypes. We also verified that RNA uptake occurred in over 90% of the cells under these transfection conditions using a nonspecific siRNA labeled with Cy3 (data not shown). Importantly, the relatively mild electroporation conditions resulted in a minimal accumulation of sub-G1/G0 cells, indicating that this RNA delivery method caused negligible cell death and is therefore suitable for performing downstream viability studies. Finally, increasing the capacitance setting or the siRNA concentration did not further increase the percentage of cells blocked in G2/M (Fig. 2b).

24 hours after transfection with two *BIM*-targeting siRNAs, steady state levels of BimEL, BimL, and BimS were markedly reduced compared to a control siRNA sequence (Fig. 3a). Neither of the *BIM*-targeting siRNAs affected expression of the housekeeping protein GAPDH (Fig. 3a), or other Bcl-2 family members Bax and Bad (data not shown). To determine if the siRNA can reduce the level of Bim even after its expression is upregulated by GC, we treated the cells with TA (100 nM) 24 h after siRNA electroporation. The 24 h recovery after electroporation allows for degradation of existing Bim protein, whose rapid turnover rate can be attributed in part to ubiquitin-proteasome processing (31). Both siRNAs caused a marked reduction in not only basal Bim expression, but also the TA-induced levels of the three major splice variants relative to a control sequence (Fig 3a, right panel). The more potent Bim siRNA (sequence 2) caused a 70 % reduction in basal BimEL (n=4) and a 30% reduction in TA-induced BimEL (n=2) (Fig. 3a, right panel, compare lanes 1 and 2 to lanes 5 and 6). To explore the RNAi effect at the mRNA level, we performed RT-PCR on total RNA isolated from siRNA-transfected 697 cells. The use of endpoint RT-PCR allows for visualization of all three major splice variants. Immediately following a 20 min post-electroporation recovery incubation (see Materials and Methods), the transfected cells were treated with vehicle or TA (100 nM), then

harvested 2.5, 5, or 7.5 h later. The mRNAs corresponding to the three major splice variants were effectively reduced by the *BIM*-targeting siRNA only 2.5 h after electroporation, and reached near-maximal silencing by that early time point as further incubation to 7.5 h had little additional effect. Treatment of the cells with TA caused *BIM* mRNA induction relative to vehicle-treated controls, which was effectively abrogated by the siRNA (Fig 3b).

To determine whether targeting Bim affects the apoptotic machinery in the 697 cells, we analyzed cells for caspase-3 activation (cleavage) and caspase-3 enzyme activity. Cells were electroporated as above, allowed to recover for 24 h (to allow for the degradation of pre-existing Bim protein), then treated with TA (5 nM) 24 h. This low, physiologically-relevant GC concentration corresponds to the approximate K_d of TA for the receptor (32). After an 18 h drug exposure, cells were immunostained with an antibody specific for the active (cleaved) form of caspase-3. Silencing of Bim reduced TA-induced caspase-3 activation, reflecting a decrease in activity of its upstream activator, caspase-9 (Fig 4a). To confirm these results, we also monitored the enzymatic activity of caspase-3 by assaying for cleavage of the fluorescent substrate, DEVD-Rhodamine-110, as described (33). *BIM* siRNA reduced GC-induced caspase-3 activity relative to the control siRNA in each of three independent transfections, averaging a 50% reduction in substrate cleavage (Fig 4b).

To determine the effect of *BIM*-targeting siRNAs on GC sensitivity, we transfected both siRNAs (#1 and #2) into the 697 cells, then treated siRNA-transfected 697 cells with TA (5 nM) 24 h after electroporation. The cells were fixed 48 h after addition of the drug (a time point chosen to result in 60% cell death, see Fig. 1a), and apoptotic cells were detected by staining with propidium iodide followed by flow cytometry (Fig. 4c). The more potent of the two sequences (#2, see Fig. 3a) decreased the percentage of cells containing sub G0/G1 by approximately 50%, while the less potent siRNA (#1) showed less of an effect. These data were also verified by Trypan blue exclusion and by staining live cells with another viability dye, 7-

aminoactinomycin-D (data not shown). Taken together, these data demonstrate that GC-mediated induction of Bim is an essential signaling event in GC-induced apoptosis in a human pre-B ALL model.

Previous work has made functional distinctions among the major Bim isoforms. In order to determine the relative contributions of BimEL, BimL and BimS in GC-induced apoptosis, we designed siRNAs that target only *BIM EL* or *BIM EL* and *BIM L*, but not *BIM S*. It is not possible to target *BIM S* independently due to the lack of a unique sequence. On the immunoblot shown in Fig. 5a, an overexposed image is shown for BimL and BimS to highlight siRNA effects on these proteins. Compared to *BIM* siRNA#2, which decreased levels of all three proteins (Fig 5a, lane 3), triplicate transfections of the two splice-variant specific siRNAs showed that these reagents successfully reduced expression of only their target isoforms. These data were corroborated by RT-PCR, which was performed 4 h after transfection (Fig. 5b). To make *BIM L* and *BIM S* mRNA more easily detectable by RT-PCR (Fig 5b), the post-electroporation recovery was performed in the presence of TA to induce their expression. To determine effects of the splice variant-specific siRNAs on GC sensitivity (Fig 5c), triplicate transfections were performed followed by a 48 h TA exposure and cell cycle analysis as in Fig. 4c. Similar to the data in Fig. 4c, the siRNA targeting all three Bim proteins reduced the percentage of sub-G0 cells from 53% to 20% (a 62% decrease in cell death). Both of the isoform-specific siRNAs also decreased GC-induced cell death, albeit to a lesser extent (39% and 36%, respectively). These data suggest that all three major splice variants contribute to GC-induced apoptosis of human pre-B ALL cells.

To explore the possibility of creating a stable cell line in which partial GC resistance is acquired through a reduction in Bim levels, we designed a short hairpin RNA (shRNA) targeting *BIM* or a control sequence. These sequences were used to produce lentiviral vectors which express shRNA under control of the H1 RNA polymerase III promoter (34). An infection rate of nearly 100% was achieved in the 697 cells, as indicated by expression of a green fluorescent

protein (GFP) marker, which is encoded by the lentivirus under control of an independent CMV promoter (Fig. 6a). GFP expression remained constant and complete in the population 8 weeks after infection, indicating that the provirus is stably integrated (data not shown). A northern hybridization using a ^{32}P-labeled probe specific for the *BIM* shRNA revealed the presence of the Dicer-processed 21-nucleotide RNA in cells infected with the *BIM* shRNA virus, but not in cells infected with a virus encoding an shRNA against firefly luciferase (Fig. 6b). In addition, the 62-nucleotide unprocessed shRNA was not detected, indicating that processing of the shRNA to the mature siRNA was rapid. Similar to the data generated with the *BIM*-targeting synthetic siRNA (Fig. 3a), immunoblot analysis revealed effective Bim silencing in both the basal state and after inducing Bim expression with TA (Fig. 6c). In addition, the *BIM* shRNA-infected cell line also effectively inhibited TA-induced caspase-3 activation (Fig. 6d).

The ratio of pro-apoptotic and anti-apoptotic Bcl-2 family members ("the Bcl-2 rheostat") (35) often controls the decision of a tumor cell to commit to irreversible intrinsic apoptosis. Bim was first isolated as a Bcl-2 binding protein (23) and its deletion prevents defects caused by Bcl-2 deficiency in mice (36). Given the previous observation that Bcl-2 (but not Bcl-XL) was reduced in response to GC in 697 cells (2), we sought to explore the role of the Bim/Bcl-2 ratio in RNAi-mediated GC resistance. We targeted *BCL2* by electroporation of synthetic siRNA, achieving a marked reduction in Bcl-2 protein (Fig. 7a). *BCL2*-targeting siRNA was then electroporated into the 697 cells stably expressing control or *BIM*-targeting shRNAs. GC sensitivity was assayed by 48 h TA exposure followed by cell cycle analysis as in previous figures (Fig. 7b). In the absence of TA, the *BCL2* siRNA had a modestly toxic effect on both lentiviral-infected cell lines. In the drug-treated cells, silencing Bcl-2 did not significantly modulate the level of GC resistance caused by *BIM* shRNA. These data suggest that Bim may function independently from Bcl-2 in GC-induced apoptosis.

Discussion

In this study, we have presented data demonstrating that GC-mediated induction of Bim is a critical signaling event in GC-induced apoptosis of human pre-B ALL cells. Under conditions where the levels of Bim proteins were reduced by 70% in the basal state and 30% in the GC-induced state (Figs. 3a and 6c), TA treatment in 697 pre-B ALL cells resulted in approximately 50% fewer apoptotic cells (Figs. 4c and 7b) as well as inhibition of caspase-3 (Figs. 4b and 6d). Using the powerful tool of splice variant-specific siRNAs, we have also demonstrated that all three major Bim proteins apparently contribute to apoptosis induction. Since GC-mediated Bim upregulation occurs in other GC-sensitive leukemic cell lines as well (namely, S49, CEM-C7 and WEHI7.2 cells) (9,27), we propose that this transcriptional event is a primary mechanism of apoptotic induction in this clinically-important signaling pathway. In this respect, this mechanism parallels many DNA damage pathways, during which p53 induces apoptosis by upregulating Noxa and Puma (37,38). Our findings do not exclude roles for other BH3-proteins in this pathway; indeed it must be noted that deletion of the *PUMA* gene causes a delayed response to dexamethasone in mouse thymocytes (39). However, *PUMA* does not appear to be a GR target gene in 697 pre-B ALL cells (7) or murine S49 T-cells (9).

Interestingly, this study suggests that Bim may be functioning independently of Bcl-2 in GC-induced apoptosis. Reducing Bcl-2 protein approximately 50% did not suppress the GC resistance caused by *BIM* shRNA. This was somewhat unexpected given the importance of the Bim/Bcl2 ratio in apoptotic pathways in a mouse knockout model (36), and the fact that Bcl-2 overexpression prevents Bim-induced cell death in mouse fibroblasts (40). The BH3-only proteins promote apoptosis by directly interacting with other Bcl-2 family members through the BH3 domain, an amphipathic α–helix that docks in a hydrophobic pocket formed by the BH1 and BH2 domains (41). Bim proteins have been shown to have the ability (a) to bind to Bcl-2,

preventing Bcl-2 from inhibiting the pro-apoptotic Bax from inserting in the mitochondrial membrane, and (b) directly to Bax, in which case they would function as direct activators of apoptosis (40). The lack of effect of the *BCL2* siRNA opens the possibility that Bim might function through Bax or Bak. Interestingly, the lymphoproliferative phenotype of $bim^{(-/-)}$ mice is similar to that of bax^{-}/bak^{-} double knockout mice (39,42). However, an alternative explanation for our result is that Bcl-2 is still in excess despite siRNA treatment, above an unachieved threshold that must be reached in order to silence the fraction that is affected by Bim binding.

While it has been established that GC regulates *BIM* mRNA transcription, there is also the possibility that GC might regulate Bim protein through post-translational mechanisms. Indeed, BimEL phosphorylation is an early event in growth factor deprivation (21). However, it is unlikely that BimEL phosphorylation is a factor in the 697 cells given that GC treatment does not affect its gel migration (Fig. 1 and unpublished observations). It has also yet to be determined whether GC treatment affects the subcellular location of BimEL and BimL, which have been shown to be released from sequestration to the dynein motor complex upon cytokine withdrawal or ultraviolet radiation exposure (25). Although Bim subcellular localization should be investigated in the future, it is worth noting that the concept of mitochondrial translocation of Bim is controversial as it has recently been shown that most of the Bim protein in healthy resting T cells is already localized to the mitochondria (26).

Previous studies demonstrated that the upregulation of *BIM* is indirect; i.e. not caused by direct binding of the GR to the *BIM* promoter. First, the promoter does not contain a glucocorticoid response element (GRE) (43). More significantly, new protein synthesis is required for *BIM* mRNA induction by GC (9). Given that a functional DNA binding GR is required for GC-induced apoptosis (44), it is likely that induction or repression of (an)other GR target gene(s) must occur as a prerequisite to the effects on Bim. Indeed, the forkhead transcription factor FHKRL1, which is known to target the *BIM* gene (45), is upregulated by GC

in 697 cells (7). However, it must be noted that targeting FHKRL1 by siRNA did not affect GC-induced apoptosis in 697 cells (unpublished observations).

Consistent with the combinatorial nature of GR-mediated transcriptional effects (46), other GR target genes might also serve as apoptotic signaling intermediates in addition to *BIM*. Although RNAi inhibition of GR target genes has not previously been reported to our knowledge, it has been reported that forced overexpression of a number of known GR target genes, including catalase (47) and *DIG2* (48) modulates the apoptotic response. Now that the GR transcriptome has been characterized by microarray experiments in numerous model systems (46), it will be possible to perform systematic RNAi screens towards uncovering the other critical signaling intermediates in this pathway. Since glucocorticoid resistance (49) and poor prognosis (50) are associated with low GR content in ALL, bypassing the receptor by targeting such downstream genes may become an effective therapeutic strategy.

Acknowledgements

We thank Dr. Gerald Litwack and Dr. Ulrich Rodeck for their advice and encouragement, Dr. Olga Igoucheva for the Northern blot analysis, Dwayne Wyre for technical assistance, and Dr. Xiao-Feng Qui and Dr. Eric Brown for the lentiviral vectors.

References

1. Planey, S. L., and Litwack, G. (2000) *Biochem Biophys Res Commun* **279**, 307-312
2. Planey, S. L., Derfoul, A., Steplewski, A., Robertson, N. M., and Litwack, G. (2002) *J Biol Chem* **277**, 42188-42196
3. Findley, H. W., Jr., Cooper, M. D., Kim, T. H., Alvarado, C., and Ragab, A. H. (1982) *Blood* **60**, 1305-1309
4. Wright, A. P., Zilliacus, J., McEwan, I. J., Dahlman-Wright, K., Almlof, T., Carlstedt-Duke, J., and Gustafsson, J. A. (1993) *J Steroid Biochem Mol Biol* **47**, 11-19
5. McConkey, D. J., Nicotera, P., Hartzell, P., Bellomo, G., Wyllie, A. H., and Orrenius, S. (1989) *Arch Biochem Biophys* **269**, 365-370
6. Cifone, M. G., Migliorati, G., Parroni, R., Marchetti, C., Millimaggi, D., Santoni, A., and Riccardi, C. (1999) *Blood* **93**, 2282-2296
7. Planey, S. L., Abrams, M. T., Robertson, N. M., and Litwack, G. (2003) *Cancer Res* **63**, 172-178
8. Medh, R. D., Webb, M. S., Miller, A. L., Johnson, B. H., Fofanov, Y., Li, T., Wood, T. G., Luxon, B. A., and Thompson, E. B. (2003) *Genomics* **81**, 543-555
9. Wang, Z., Malone, M. H., He, H., McColl, K. S., and Distelhorst, C. W. (2003) *J Biol Chem* **278**, 23861-23867
10. Alnemri, E. S., Fernandes, T. F., Haldar, S., Croce, C. M., and Litwack, G. (1992) *Cancer Res* **52**, 491-495
11. Borner, C. (2003) *Mol Immunol* **39**, 615-647
12. Yip, K. W., Li, A., Li, J. H., Shi, W., Chia, M. C., Rashid, S. A., Mocanu, J. D., Louie, A. V., Sanchez, O., Huang, D., Busson, P., Yeh, W. C., Gilbert, R., O'Sullivan, B., Gullane, P., and Liu, F. F. (2004) *Mol Ther* **10**, 533-544
13. Yamaguchi, T., Okada, T., Takeuchi, K., Tonda, T., Ohtaki, M., Shinoda, S., Masuzawa, T., Ozawa, K., and Inaba, T. (2003) *Gene Ther* **10**, 375-385
14. Bouillet, P., Metcalf, D., Huang, D. C., Tarlinton, D. M., Kay, T. W., Kontgen, F., Adams, J. M., and Strasser, A. (1999) *Science* **286**, 1735-1738
15. Egle, A., Harris, A. W., Bouillet, P., and Cory, S. (2004) *Proc Natl Acad Sci U S A* **101**, 6164-6169
16. Shinjyo, T., Kuribara, R., Inukai, T., Hosoi, H., Kinoshita, T., Miyajima, A., Houghton, P. J., Look, A. T., Ozawa, K., and Inaba, T. (2001) *Mol Cell Biol* **21**, 854-864
17. Putcha, G. V., Moulder, K. L., Golden, J. P., Bouillet, P., Adams, J. A., Strasser, A., and Johnson, E. M. (2001) *Neuron* **29**, 615-628
18. Villunger, A., Marsden, V. S., Zhan, Y., Erlacher, M., Lew, A. M., Bouillet, P., Berzins, S., Godfrey, D. I., Heath, W. R., and Strasser, A. (2004) *Proc Natl Acad Sci U S A* **101**, 7052-7057
19. Sunters, A., Fernandez de Mattos, S., Stahl, M., Brosens, J. J., Zoumpoulidou, G., Saunders, C. A., Coffer, P. J., Medema, R. H., Coombes, R. C., and Lam, E. W. (2003) *J Biol Chem* **278**, 49795-49805
20. Marani, M., Hancock, D., Lopes, R., Tenev, T., Downward, J., and Lemoine, N. R. (2004) *Oncogene* **23**, 2431-2441
21. Reginato, M. J., Mills, K. R., Paulus, J. K., Lynch, D. K., Sgroi, D. C., Debnath, J., Muthuswamy, S. K., and Brugge, J. S. (2003) *Nat Cell Biol* **5**, 733-740
22. Kuribara, R., Honda, H., Matsui, H., Shinjyo, T., Inukai, T., Sugita, K., Nakazawa, S., Hirai, H., Ozawa, K., and Inaba, T. (2004) *Mol Cell Biol* **24**, 6172-6183
23. O'Connor, L., Strasser, A., O'Reilly, L. A., Hausmann, G., Adams, J. M., Cory, S., and Huang, D. C. (1998) *Embo J* **17**, 384-395
24. Chen, D., and Zhou, Q. (2004) *Proc Natl Acad Sci U S A* **101**, 1235-1240

25. Puthalakath, H., Huang, D. C., O'Reilly, L. A., King, S. M., and Strasser, A. (1999) *Mol Cell* **3**, 287-296
26. Zhu, Y., Swanson, B. J., Wang, M., Hildeman, D. A., Schaefer, B. C., Liu, X., Suzuki, H., Mihara, K., Kappler, J., and Marrack, P. (2004) *Proc Natl Acad Sci U S A* **101**, 7681-7686
27. Zhang, L., and Insel, P. A. (2004) *J Biol Chem* **279**, 20858-20865
28. Scherr, M., Morgan, M. A., and Eder, M. (2003) *Curr Med Chem* **10**, 245-256
29. Paddison, P. J., Caudy, A. A., Sachidanandam, R., and Hannon, G. J. (2004) *Methods Mol Biol* **265**, 85-100
30. Weil, D., Garcon, L., Harper, M., Dumenil, D., Dautry, F., and Kress, M. (2002) *Biotechniques* **33**, 1244-1248
31. Ley, R., Balmanno, K., Hadfield, K., Weston, C., and Cook, S. J. (2003) *J Biol Chem* **278**, 18811-18816
32. Zhang, S., and Danielsen, M. (1995) *Recent Prog Horm Res* **50**, 429-435
33. Liu, J., Bhalgat, M., Zhang, C., Diwu, Z., Hoyland, B., and Klaubert, D. H. (1999) *Bioorg Med Chem Lett* **9**, 3231-3236
34. Abbas-Terki, T., Blanco-Bose, W., Deglon, N., Pralong, W., and Aebischer, P. (2002) *Hum Gene Ther* **13**, 2197-2201
35. Renner, K., Ausserlechner, M. J., and Kofler, R. (2003) *Curr Mol Med* **3**, 707-717
36. Bouillet, P., Cory, S., Zhang, L. C., Strasser, A., and Adams, J. M. (2001) *Dev Cell* **1**, 645-653
37. Shibue, T., Takeda, K., Oda, E., Tanaka, H., Murasawa, H., Takaoka, A., Morishita, Y., Akira, S., Taniguchi, T., and Tanaka, N. (2003) *Genes Dev* **17**, 2233-2238
38. Nakano, K., and Vousden, K. H. (2001) *Mol Cell* **7**, 683-694
39. Villunger, A., Michalak, E. M., Coultas, L., Mullauer, F., Bock, G., Ausserlechner, M. J., Adams, J. M., and Strasser, A. (2003) *Science* **302**, 1036-1038
40. Marani, M., Tenev, T., Hancock, D., Downward, J., and Lemoine, N. R. (2002) *Mol Cell Biol* **22**, 3577-3589
41. Puthalakath, H., and Strasser, A. (2002) *Cell Death Differ* **9**, 505-512
42. Lindsten, T., Ross, A. J., King, A., Zong, W. X., Rathmell, J. C., Shiels, H. A., Ulrich, E., Waymire, K. G., Mahar, P., Frauwirth, K., Chen, Y., Wei, M., Eng, V. M., Adelman, D. M., Simon, M. C., Ma, A., Golden, J. A., Evan, G., Korsmeyer, S. J., MacGregor, G. R., and Thompson, C. B. (2000) *Mol Cell* **6**, 1389-1399
43. Bouillet, P., Zhang, L. C., Huang, D. C., Webb, G. C., Bottema, C. D., Shore, P., Eyre, H. J., Sutherland, G. R., and Adams, J. M. (2001) *Mamm Genome* **12**, 163-168
44. Reichardt, H. M., Kaestner, K. H., Tuckermann, J., Kretz, O., Wessely, O., Bock, R., Gass, P., Schmid, W., Herrlich, P., Angel, P., and Schutz, G. (1998) *Cell* **93**, 531-541
45. Gilley, J., Coffer, P. J., and Ham, J. (2003) *J Cell Biol* **162**, 613-622
46. Rogatsky, I., Wang, J. C., Derynck, M. K., Nonaka, D. F., Khodabakhsh, D. B., Haqq, C. M., Darimont, B. D., Garabedian, M. J., and Yamamoto, K. R. (2003) *Proc Natl Acad Sci U S A* **100**, 13845-13850
47. Tome, M. E., Lutz, N. W., and Briehl, M. M. (2003) *Biochim Biophys Acta* **1642**, 149-162
48. Wang, Z., Malone, M. H., Thomenius, M. J., Zhong, F., Xu, F., and Distelhorst, C. W. (2003) *J Biol Chem* **278**, 27053-27058
49. Tissing, W. J., Meijerink, J. P., den Boer, M. L., and Pieters, R. (2003) *Leukemia* **17**, 17-25
50. Kato, G. J., Quddus, F. F., Shuster, J. J., Boyett, J., Pullen, J. D., Borowitz, M. J., Whitehead, V. M., Crist, W. M., and Leventhal, B. G. (1993) *Blood* **82**, 2304-2309

Figure Legends

Figure 1. GC sensitivity and Bim induction in human pre-B ALL cell lines.
A, B, The cell lines 697 (triangles), Nalm-6 (closed circles), Kasumi-2 (open circles), and Kopn-8 (squares) were treated with 0.5-500 nM TA for 48 h (*A*) or 72 h (*B*) and assayed for cell viability by Trypan blue exclusion. Error bars represent the SEM of three assays. *C*, The panel of pre-B ALL cells was treated with vehicle or 100 nM TA for 24 h and whole cell lysates were immunoblotted with Bim and GAPDH antibodies. The positions of the three major Bim proteins are indicated. *D*, The 697 cell line was treated with vehicle or 100 nM TA for 4 or 8 hours and immunoblotted as in *C*.

Figure 2. **Optimization of siRNA electroporation in 697 cells.** *A*, Cells were electroporated with siRNAs targeting firefly luciferase ("Ctrl siRNA") or KSP at 200 V / 500 μF. The cells were fixed after 48 h and subjected to propidium iodide staining and flow cytometry. The G1 and G2/M peaks of the cell cycle are indicated. *B*, Quantitation of cells in G2/M arrest after electroporating cells with control (white bars) or KSP (black bars) siRNAs under different conditions, representative of two trials.

Figure 3. *BIM*-targeting siRNAs reduce basal and GC-induced BimEL, BimL and BimS proteins and the corresponding mRNAs in 697 pre-B ALL cells. *A*, Cells were transfected with two unique *BIM* siRNA sequences (*BIM*#1 and *BIM*#2) and the control luciferase siRNA ("Ctrl"). For the experiment shown in the left panel, cells were harvested and lysed 24 h after transfection. Right panel, cells were treated with vehicle or 100 nM TA as indicated 24 h after transfection and harvested after a 24 h treatment. The densitometry data for BimEL are above

the image. Both siRNAs reduced the basal as well as the TA-induced protein levels and that *BIM*#2 is more potent of the two RNA duplexes. *B*, Cells were treated with vehicle or 100 nM TA for 2.5, 5, or 7.5 h immediately after transfection with *BIM*-targeting siRNA (*BIM*#1). Total RNA was isolated and subjected to RT-PCR using primers specific for *BIM* (left) or *GAPDH* (right). The positions of the three major splice variants are indicated.

Figure 4. *BIM* siRNA inhibits GC-induced caspase-3 activity and confers partial resistance to GC in 697 cells. *A*, Cells were transfected with control (left) or *BIM* (right) siRNAs, followed 24 h later by treatment with 5 nM TA. After an additional 24 h, cells were spun onto microscope slides, fixed, permeabilized, and subjected to immunofluorescence using an antibody specific for cleaved (activated) caspase-3. Bound antibody was detected with AlexaFluor 488 (green) and nuclei were counterstained with DAPI (blue). *B***,** Cells were transfected and treated with vehicle or TA as above, followed by cell lysis and assayed for cleavage of the fluorescent caspase-3 substrate DEVD-Rhodamine-110. Error bars represent SEM of three assays. *C*, Triplicate transfections with the control siRNA (white bars), *BIM*#1 siRNA (striped bars), or *BIM*#2 siRNA (black bars), followed 24 h later by addition of vehicle or 5 nM TA was performed as above. Cells were fixed after a 48 h treatment and subjected to propidium iodide staining and flow cytometry. Apoptotic (sub-G0) cells were scored using WinMDI software. Error bars represent the SEM of three measurements, each originating from an independent siRNA transfection.

Figure 5. Generation of splice variant-specific *BIM* siRNAs. *A*, siRNA duplexes specific for *BIM* splice variants were designed and transfected in triplicate, followed 24 h later by immunoblotting with anti-Bim and anti-GAPDH antibodies. siRNAs used in this experiment targeted firefly luciferase ("Ctrl", lanes 1 and 2), all three major splice variants ("all", *BIM* si#2,

lane 3), BimEL only (lanes 4-6), or BimEL + BimL (lanes 7-9). *B*, Cells were transfected as above, immediately followed by treatment with 100 nM TA. Cells were harvested after 4 hours and subjected to RT-PCR using primers specific for *BIM* or *GAPDH* as in Fig. 3b. *C*, siRNAs were assayed for effect on GC sensitivity as in Fig. 4c. Control (luciferase), white bars; *BIM* si#2, black; BimEL-only siRNA, striped; BimEL+BimL siRNA, dotted.

Figure 6. Lentiviral delivery of Bim shRNA. *A*, The 697 cells were infected with a lentivirus encoding Bim shRNA and analyzed by fluorescence microscopy after 48 h for expression of green fluorescent protein (GFP). *B,* Total RNA (30 μg) from cells infected with lentivirus encoding Bim ("Bim") or control ("Ctrl", luciferase) shRNAs was subjected to northern hybridization with a probe complementary to the antisense strand of Bim shRNA. The gel was stained with ethidium bromide ("EtBr") as a loading control before transfer. PM (perfect match), control oligonucleotide with complete complementarity to the probe; MM (mismatch), control oligonucleotide which is complementary to the probe except for two mismatched bases. *C*, Cell lines stably expressing control or Bim shRNAs were analyzed for effects on basal (left image) and TA-induced (right) Bim protein levels by immunoblot. Each cell line was treated with vehicle, 5, or 100 nM TA as indicated and the densitometry data for BimEL (above image) show that the *BIM* shRNA-expressing cells induced Bim protein to a level that was >30% lower than the control siRNA. *D*, Control (white bars) and *BIM* shRNA (black bars) expressing cells were subject to caspase-3 activity assay after 24 h vehicle or TA treatment as in Fig. 4b.

Figure 7. Effect of reducing Bcl-2 protein levels on GC resistance caused by *BIM* shRNA. *A*, Three siRNAs targeting *BCL2* mRNA were tested on 697 cells (as in Fig. 3a) and protein extracts were immunoblotted using antibodies against Bcl-2 and GAPDH. *B*, Cells stably expressing control shRNA (solid bars) or *BIM* shRNA (dotted bars) were transfected with

control siRNA (white bars) or *BCL2* siRNA (*BCL2*#1, black bars) followed by a 48 h vehicle or TA treatment as in Figs. 4c and 5c. Error bars represent the SEM of three assays.

Figure 1

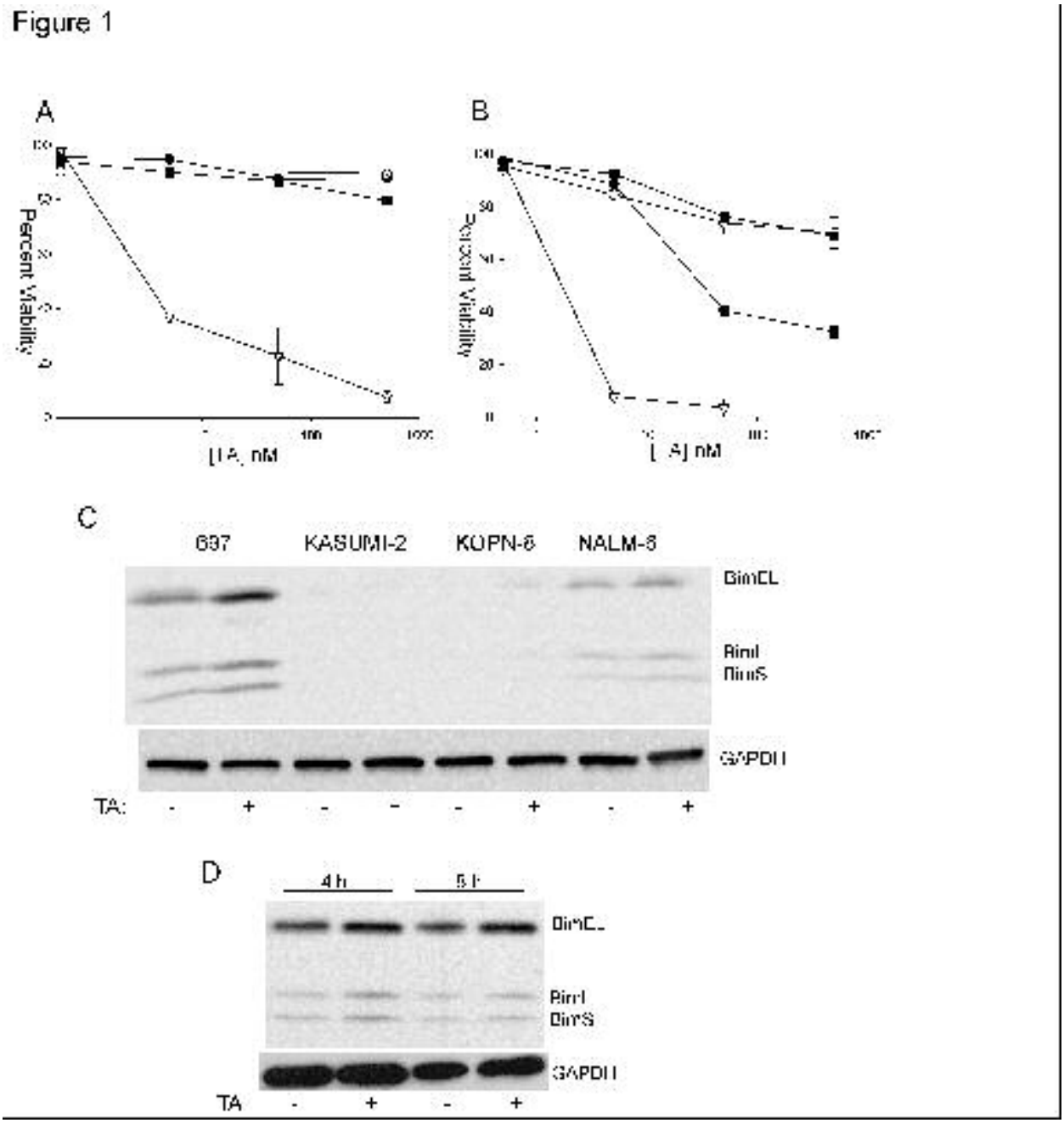
A
Percent Viability
[TA], nM
B
Percent Viability
[A] nM
C
697
KASUMI-2
KOPN-8
NALM-6
BimEL
BimL
BimS
GAPDH
TA:
D
4 h
BimEL
BimL
BimS
GAPDH
TA

Figure 2

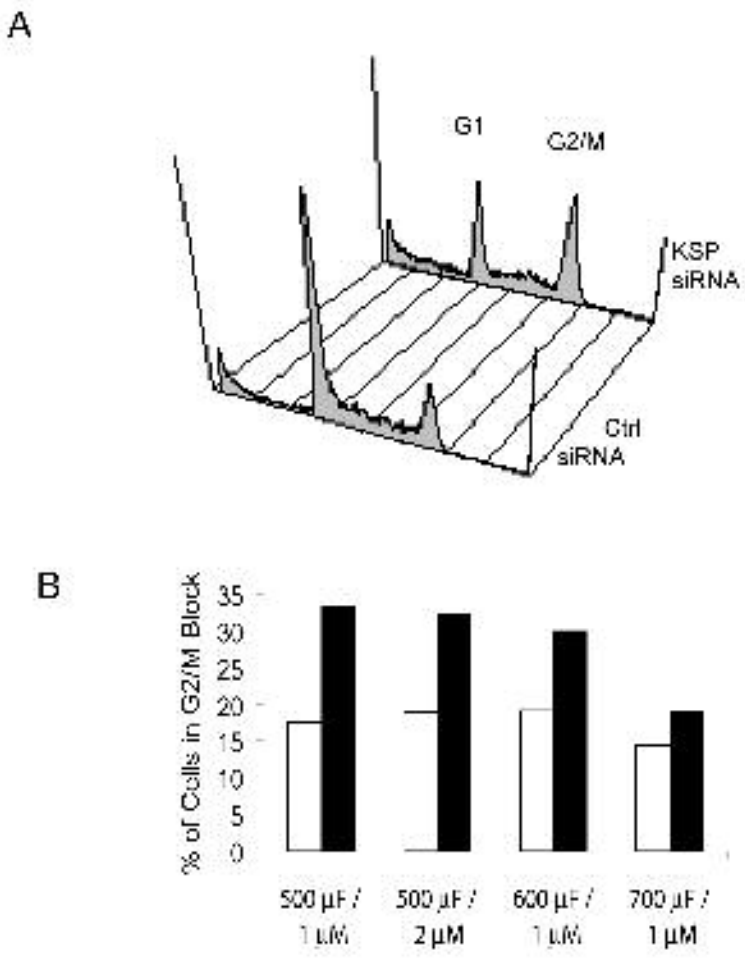
A
G1
G2/M
KSP siRNA
Ctrl siRNA
B
% of Cells in G2/M Block
35
30
25
20
15
10
5
0
500 µF / 1 µM
500 µF / 2 µM
600 µF / 1 µM
700 µF / 1 µM

Figure 3

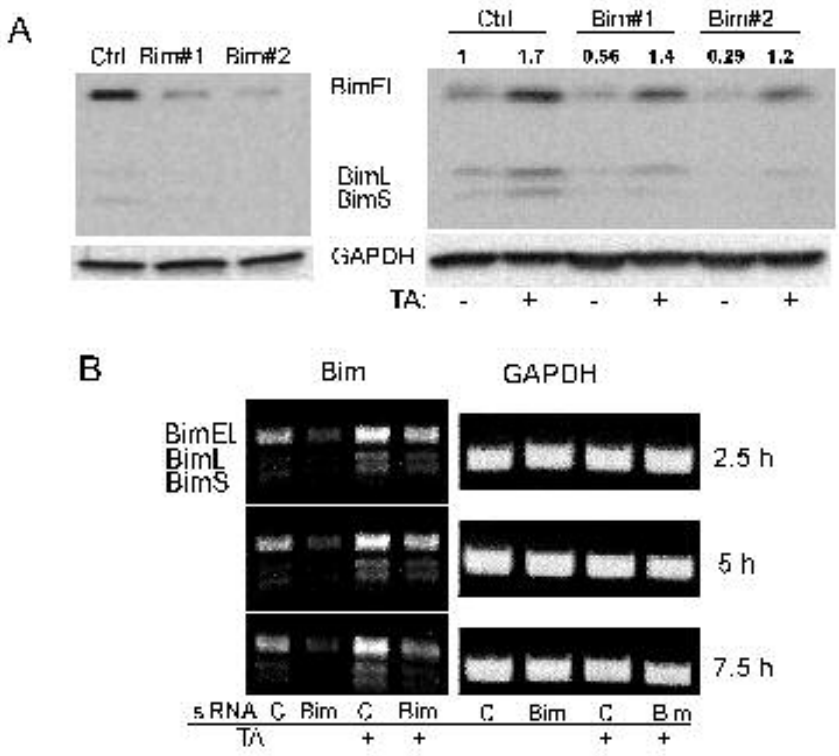
A
Ctrl Bim#1 Bim#2
Ctrl Bim#1 Bim#2
1 1.7 0.56 1.4 0.29 1.2
BimEl
BimL
BimS
GAPDH
TA: - + - + - +
B
Bim
GAPDH
BimEL
BimL
BimS
2.5 h
5 h
7.5 h
siRNA C Bim C Bim C Bim C Bim
TA + + + +

Figure 4

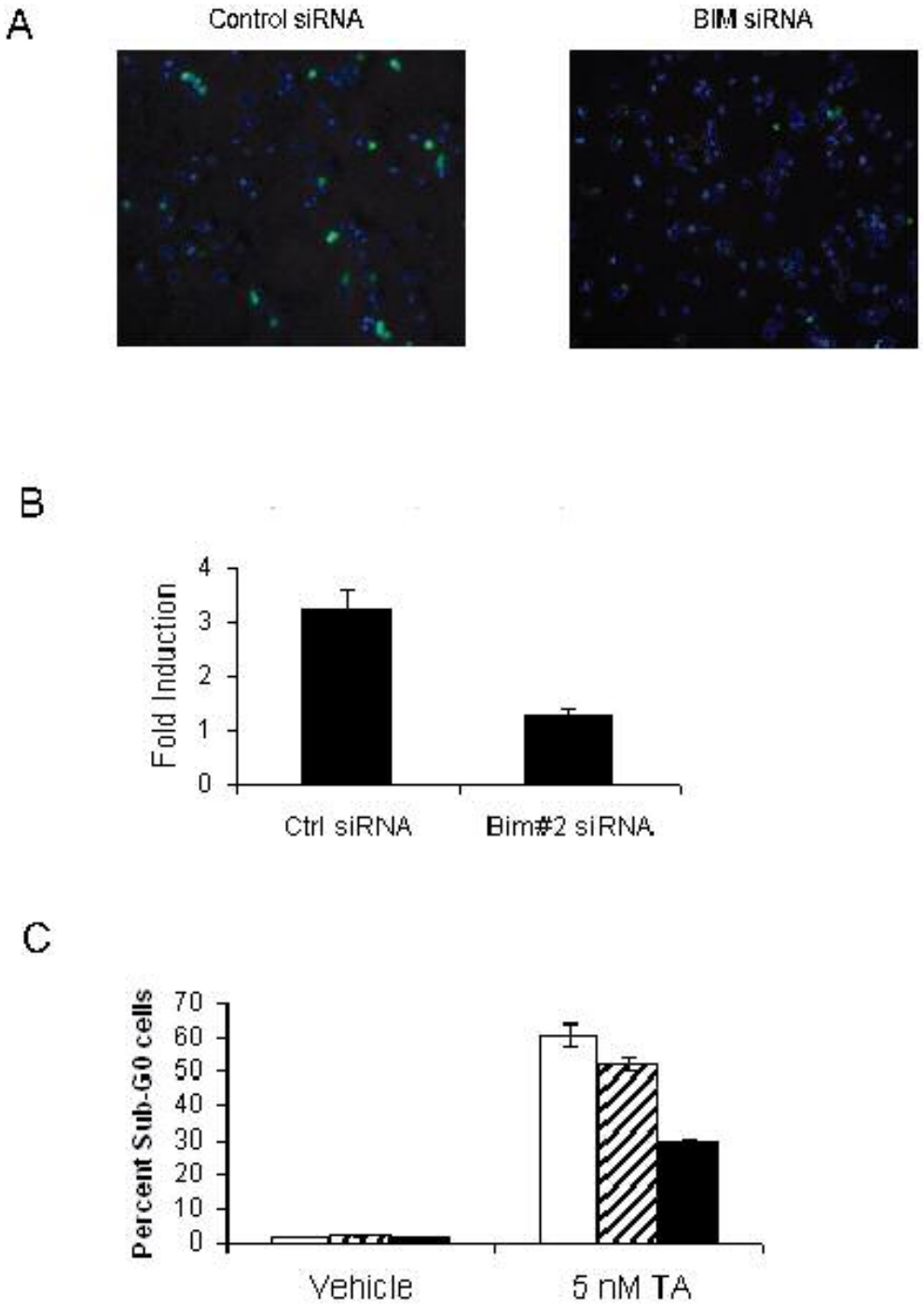
A
Control siRNA
BIM siRNA
B
Fold Induction
0
1
2
3
4
Ctrl siRNA
Bim#2 siRNA
C
Percent Sub-G0 cells
0
10
20
30
40
50
60
70
Vehicle
5 nM TA

Figure 5

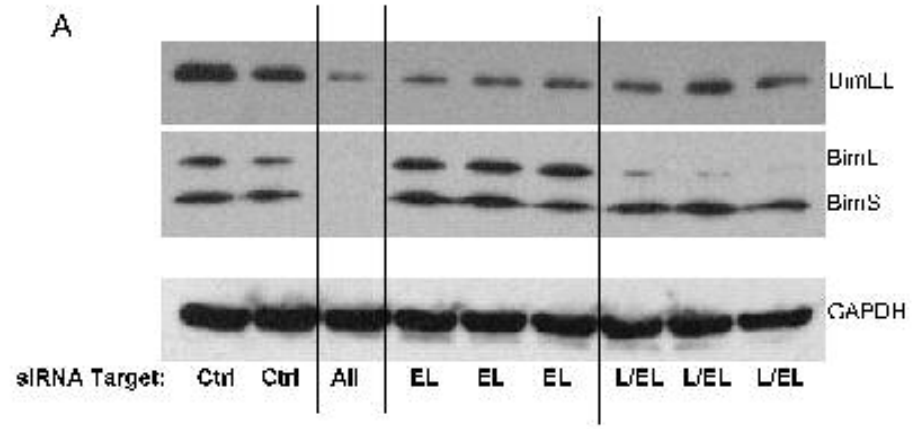
A
UmLL
BimL
BimS
GAPDH
siRNA Target: Ctrl Ctrl All EL EL EL L/EL L/EL L/EL

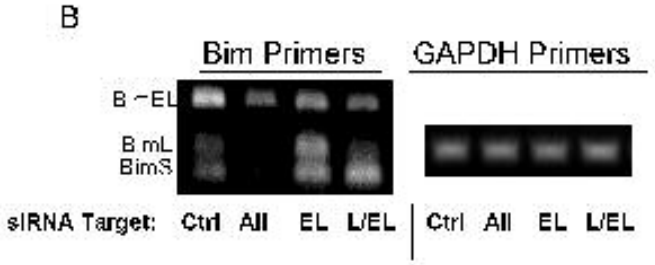
B
Bim Primers
GAPDH Primers
B mL
BimS
siRNA Target: Ctrl All EL L/EL Ctrl All EL L/EL

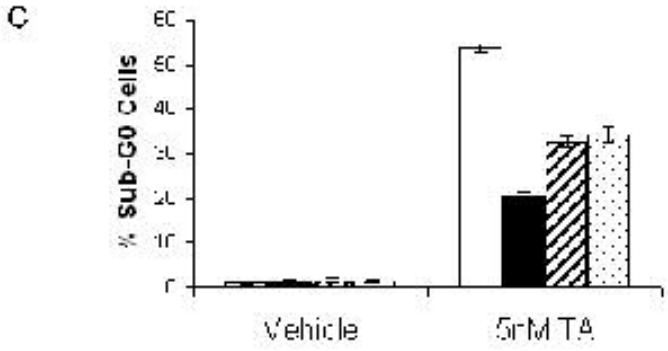
C
% Sub-G0 Cells
Vehicle
5nM TA

Figure 6

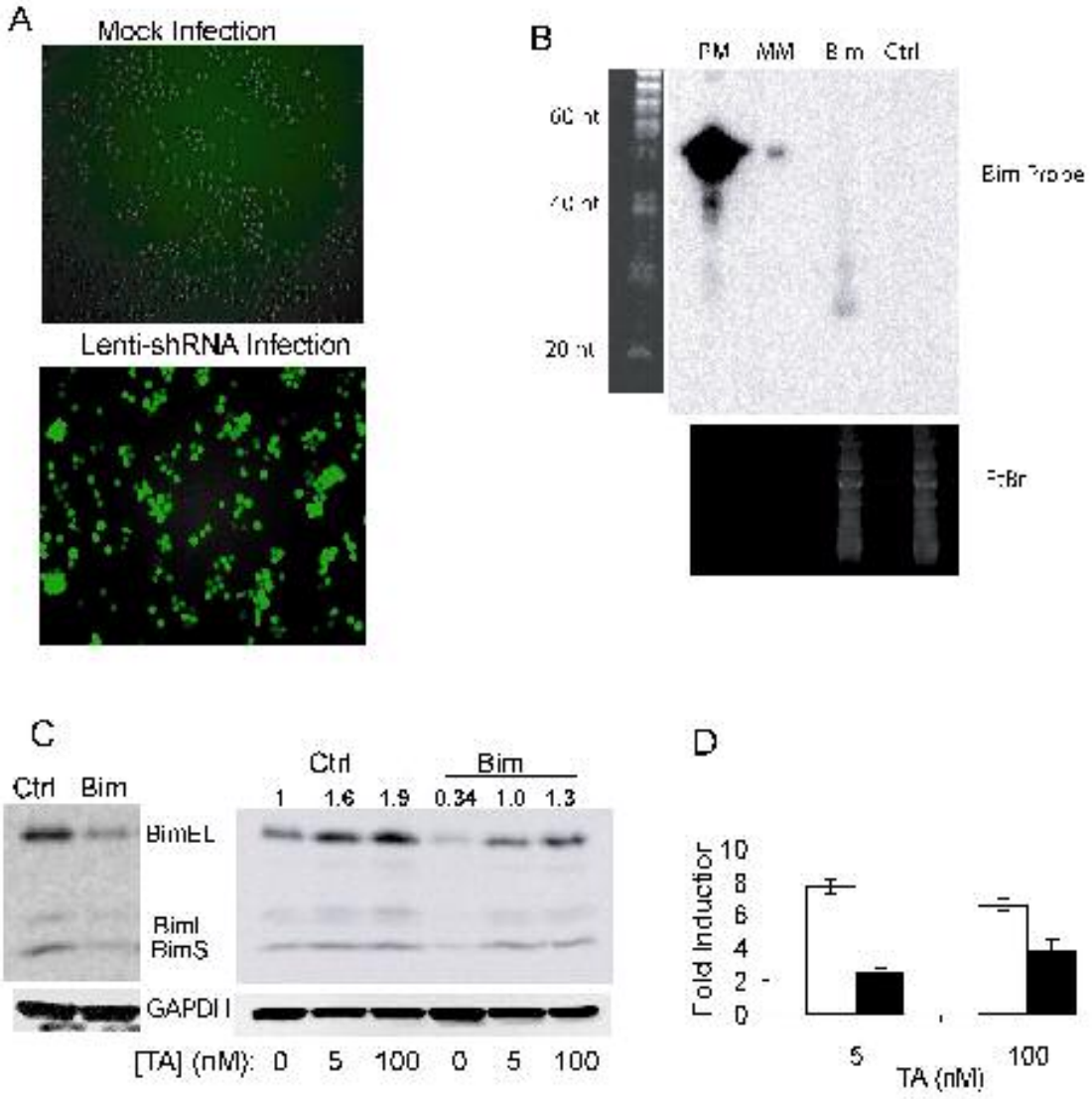
A
Mock Infection
Lenti-shRNA Infection
B
PM
MM
Bim
Ctrl
60 nt
40 nt
20 nt
Bim Probe
EtBr
C
Ctrl
Bim
Ctrl
Bim
1
1.6
1.9
0.34
1.0
1.3
BimEL
BimL
BimS
GAPDH
[TA] (nM): 0 5 100 0 5 100
D
Fold Induction
10
8
6
4
2
0
5
100
TA (nM)

Figure 7

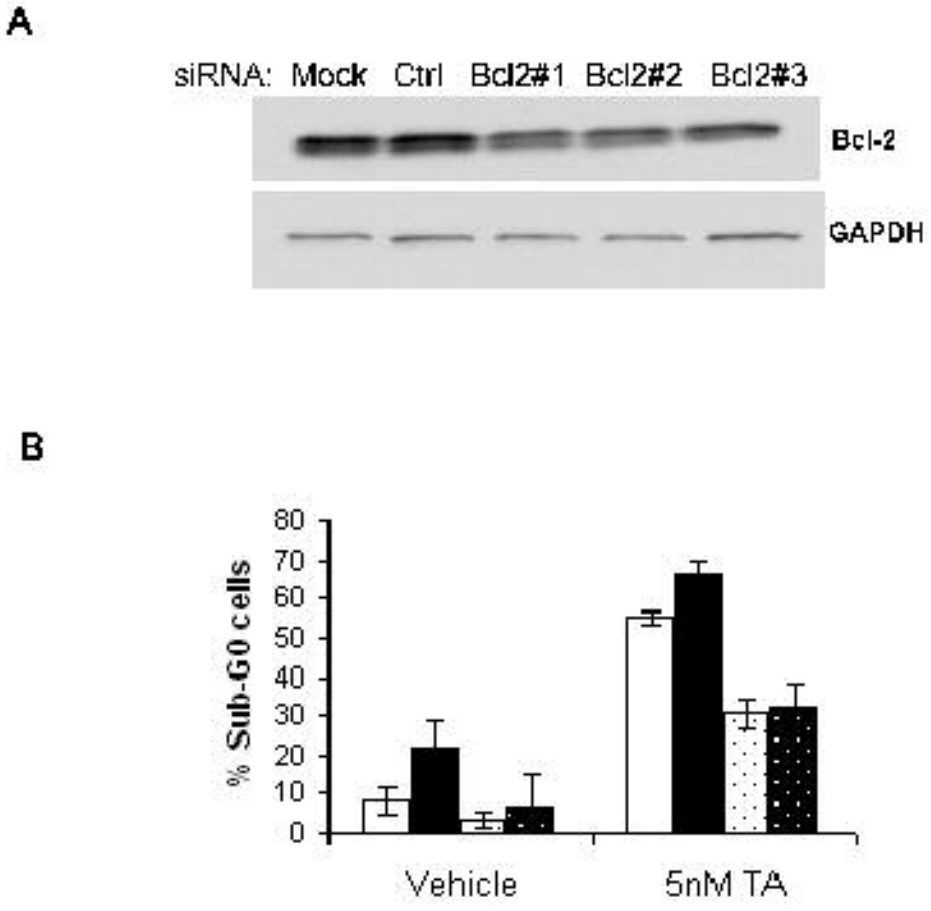
A
siRNA: Mock Ctrl Bcl2#1 Bcl2#2 Bcl2#3
Bcl-2
GAPDH
B
% Sub-G0 cells
80
70
60
50
40
30
20
10
0
Vehicle
5nM TA